

# Multi-Parameter Optical Fiber Sensing of Gaseous Ammonia and Carbon Dioxide

LiangLiang Liu , Stephen P. Morgan , Ricardo Correia, Seung-Woo Lee, and Serhiy Korposh 

**Abstract**—Ammonia (NH<sub>3</sub>) and carbon dioxide (CO<sub>2</sub>) are important breath biomarkers for diagnosis of renal and respiratory diseases. Simultaneous sensing of the two gases is useful for assessment of *Helicobacter Pylori* infection. This article introduces a multi-parameter optical fibre sensor by coating two different dyes, i.e., thymol blue and tetraphenylporphyrin tetrasulfonic acid hydrate (TPPS) into one optical fibre sensing system for multi-sensing of the two gases. The dyes are separately coated on distal ends of a 2 × 2 optical fibre coupler using the sol-gel technique. The reflection spectrum contains distinctive absorption peaks of the two dyes in the wavelength domain and hence can be analysed using a single spectrometer. The absorbance at a wavelength of 608 nm corresponding to the absorption peak of the thymol blue exhibits an exponential decrease as the CO<sub>2</sub> concentration increases from 0 ppm to 60 000 ppm. The absorption bands at approximately 490 nm and 711 nm corresponding to the Soret band and Q-band of TPPS, respectively, show changes both in absorbance and central wavelengths in response to NH<sub>3</sub> concentration in the range from 0 ppm to 80 ppm. The limit of detection and response time for CO<sub>2</sub> and NH<sub>3</sub> are 637 ppm and 0.15 ppm, 86 s and 83 s, respectively. The proposed sensor demonstrates the capability of sensing NH<sub>3</sub> and CO<sub>2</sub> simultaneously in a complex gas atmosphere containing other chemicals such as methanol and acetone, which are representative of industrial or metabolic compounds that may confound measurements.

**Index Terms**—Gas sensing, multi-parameter sensing, optical fibre sensor, pH dyes.

## I. INTRODUCTION

THE use of an optical fibre sensor (OFS) for chemical sensing has become a popular approach both in scientific research and in commercial applications [1]–[4] owing to the high sensitivity, small size, flexibility and ability to multiplex a number of sensors. An optical fibre based sensing platform is intrinsically immune to electromagnetic interference and can be deployed in a harsh corrosive environment due to the chemically inert substrate of a silica fibre. An OFS usually inherits the

Manuscript received September 29, 2019; revised November 7, 2019; accepted November 9, 2019. Date of publication November 13, 2019; date of current version April 1, 2020. This work was supported by the Medical Research Council, U.K. under Grant MR/R025266/1. (Corresponding author: LiangLiang Liu.)

L. Liu, S. P. Morgan, R. Correia, and S. Korposh are with the Optics and Photonics Group, University of Nottingham, Nottingham NG7 2RD, U.K. (e-mail: liangliang.liu1@nottingham.ac.uk; steve.morgan@nottingham.ac.uk; ricardo.goncalvescorreia@nottingham.ac.uk; s.korposh@nottingham.ac.uk).

S.-W. Lee is with the Graduate School of Environmental Engineering, University of Kitakyushu, Kitakyushu 802-8577, Japan (e-mail: leesw@kitakyu-u.ac.jp).

Color versions of one or more of the figures in this article are available online at <http://ieeexplore.ieee.org>.

Digital Object Identifier 10.1109/JLT.2019.2953271

geometrical property of an optical fibre that is typically  $\sim 125 \mu\text{m}$  in diameter and requires only a small volume size of the sample for measurement. Applications of interest include healthcare [5], environmental monitoring [6] and bioprocess monitoring [7].

Chemical sensing with an OFS usually relies on a change of optical absorption [2], fluorescence [3], refractive index [4] of a sensing element (or chemical transducer) while interacting with target analytes. An OFS can provide multi-parameter sensing and this is commonly achieved by using optical fibre gratings such as a long period fibre grating (LPG) or a fibre Bragg grating (FBG) as they provide wavelength multiplexing capabilities [8], [9]. Multi-parameter sensing can also be achieved by fabricating multiple sensors on the fibre tip that report each analyte separately [10], [11]. Such sensors are attractive as they take the cross-section of an optical fibre as a substrate and measurements of the absorption or reflection from the tip of the fibre also offers a simple measurement approach. The drawback of such sensors is that it is challenging to make accurate measurements of the intensity at the tip of the fibre due to systematic errors such as fibre bending losses and drift of the light source. A factor to consider with all chemical sensors is cross sensitivity due to a second species interfering with the target analyte. The signals due to each analyte need to be differentiated when two sensitive parameters change at the same time.

Ammonia (NH<sub>3</sub>) and carbon dioxide (CO<sub>2</sub>) are important gases for assessing indoor air quality as exceeding the exposure limit will result in health issues for people remaining in this environment [12]. For example, swine workers in livestock buildings are at risk of developing respiratory diseases as a result of exposure to CO<sub>2</sub>, NH<sub>3</sub> and dust which are the main sources of the indoor air contamination [13]. The long-term exposure limit (up to 10 hours) for CO<sub>2</sub> and NH<sub>3</sub> are regulated at 5,000 ppm and 25 ppm respectively according to the Occupational Safety and Health Administration (OSHA) [14]. NH<sub>3</sub> and CO<sub>2</sub> are also important breath biomarkers for diagnosis of renal [15] and respiratory [16] diseases respectively. In some diseases such as *Helicobacter Pylori* infection, both gases are produced simultaneously [17]. Breath gas contains CO<sub>2</sub> ( $\sim 5\%$  in concentration), water vapour (saturated at 37 °C about 6%) as well as a mixture of over 500 kinds of components including volatile organic and inorganic metabolites such as NH<sub>3</sub> (833 ppb), acetone (4 ppb) and methanol (461 ppb) [18]. The analysis of breath gas provides valuable information about the physiological and pathophysiological condition of a patient [19], [20]. Gas chromatography combined with mass spectrometry (GC-MS) provides a reliable and sensitive method for breath analysis in measuring the two

gases [18]. Despite its high sensitivity, GC-MS has considerable drawbacks due to the high cost and non-portable feature.

Sensing of  $\text{CO}_2/\text{NH}_3$  by using OFSs has been conducted separately in most cases and pH indicators based on the colorimetric sensing method are commonly used [21]–[23]. In these cases, the  $\text{CO}_2/\text{NH}_3$  reacts with water molecules preserved in the same matrix film to produce hydrogen ions ( $\text{H}^+$ )/hydroxide ions ( $\text{OH}^-$ ) which protonate /deprotonate the pH indicators resulting in a change in the absorption spectrum of the film.  $\text{NH}_3$  can also directly interact with indicators like tetrakis-(4-sulfophenyl) porphine (TSPP or TPPS) leading to a deprotonation process utilised in OFS development [24]. The pH indicator based sensors generally do not specifically respond to any class of gases as both acid and alkaline gases (i.e.,  $\text{CO}_2$  and  $\text{NH}_3$ ) change the pH value. However, the sensitivity of such OFSs highly depends on the acid dissociation constant (pKa) value of pH indicators as well as the solubility of the gases in the matrix film. By carefully selecting the dye and matrix film, pH indicators based OFS can be fabricated with low cross sensitivity. Porous silica film is chosen in this work as the matrix film for doping sensitive dyes due to its excellent mechanical properties over general polymer based matrix films, and it attaches strongly to the silica optical fibres.

In this paper, an integrated OFS that is capable of measuring gaseous  $\text{CO}_2$  and  $\text{NH}_3$  simultaneously by using two pH-sensitive dyes (thymol blue and TPPS) is, to the best of our knowledge, reported for the first time. The novelty also includes the reflection mode for sensing of  $\text{NH}_3$  by using TPPS. As the two dyes operate at different pH ranges for sensing of  $\text{CO}_2$  and  $\text{NH}_3$ , the general procedure of one single sensing region cannot be applied. Therefore, the final sensor configuration is determined as a two-film structure in which the two dyes are doped inside two separate sol-gel films and coated individually on the two distal ends of a  $2 \times 2$  optical fibre coupler (3 dB,  $62.5 \mu\text{m}$  in core diameter). The two-tip configuration provides flexibility of being a single compact sensor to measure the two gases locally in a small volume and being a spatial multiplexing sensor to measure the two gases in different locations. The reflection spectrum contains the absorption peaks of the two dyes that have no interference with each other at the selected wavelength. The selected wavelengths show no cross-talk between the two gases and demonstrate the ability to sense  $\text{NH}_3$  and  $\text{CO}_2$  simultaneously in the presence of other breath gases, i.e., methanol and acetone.

## II. MATERIALS AND METHODS

### A. Materials

Methyltriethoxysilane (MTEOS), thymol blue, ethanol and tetramethylammonium hydroxide (TMAH) solution (10% in water), hydrochloric acid (HCl) (37%), ammonium hydroxide solution ( $\text{NH}_4\text{OH}$ ) (28%), acetone and methanol were purchased from Sigma-Aldrich, UK. Tetraphenylporphyrin tetrasulfonic acid hydrate (TPPS) was purchased from Tokyo Chemical Industry, UK. Carbon dioxide (5% in argon mixture) was purchased from Ryvalgas, UK. Nitrogen (oxygen-free) was purchased from BOC, UK.

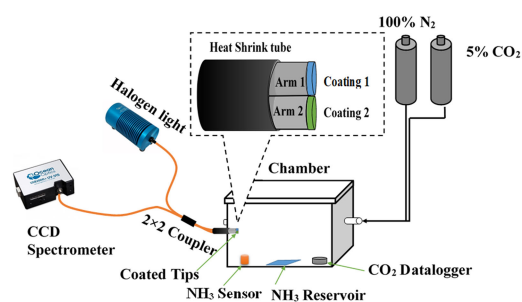


Fig. 1. Experimental set-up of the sensor calibration; the two tips of the OFS were coated with two different films for sensing of  $\text{CO}_2$  and  $\text{NH}_3$ , respectively. (Inset) Two tips coated with functional films packed inside a heat shrink tube.

### B. Preparation of the Optical Fibre Sensor

*Coating solution 1* (for  $\text{CO}_2$  sensing): 2 mL MTEOS, 5 mL Ethanol, 23 mg thymol blue are mixed under stirring at room temperature ( $\sim 22^\circ\text{C}$ ) for about 10 mins, then 0.5 mL of TMAH is added into the solution mixture and stirring is maintained for 2 hours prior to use.

*Coating solution 2* (for  $\text{NH}_3$  sensing): 2 mL MTEOS, 5 mL ethanol, 1 mL distilled water and  $0.5 \mu\text{L}$  HCl is added into a capped clean glass beaker under stirring and heating ( $50^\circ\text{C}$ ) for approximate 10 mins, and then 7 mg TPPS is added into the solution mixture and the reaction is maintained for 30 mins.

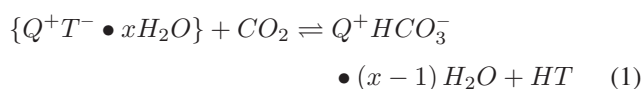
Two distal ends of the optical fibre coupler (3 dB, F-CPL-M22855, Newport, UK) are cleaved at 90 degrees for dip coating using an in-house built dip coater. One tip of the arm is dip coated using the *coating solution 1* with a withdrawal speed of 6 mm/s. The procedure is repeated 4 times with 2 mins drying period between each coating to obtain sufficient absorption after drying for sensing of  $\text{CO}_2$  [23]. Another tip is dip coated once with the *coating solution 2* with a withdrawal speed of 6 mm/s that provides sufficient absorption for sensing of  $\text{NH}_3$ . The coated fibres are then dried in ambient conditions for 24 hours before use. The two arms are packaged into a heat shrink tube so that the two tips are close to each other (illustrated in Fig. 1) and will be exposed simultaneously to the analyte gases.

### C. Experimental Set-Up and Sensor Characterisation

The sensor response to  $\text{CO}_2$  and  $\text{NH}_3$  was conducted by using the same experimental set-up shown in Fig. 1. A halogen light source (HL-2000, Ocean Optics, Germany) and a CCD spectrometer (USB 2000+, Ocean Optics, Germany) are used as the light source and detector to obtain spectral information of the coated films from the tips of the optical fibre coupler. Calibration of the sensor was done by placing the coated tips in an in-house built acrylic gas measurement chamber ( $15 \text{ cm(L)} \times 13 \text{ cm(W)} \times 8 \text{ cm(H)}$ ) which has a  $\text{CO}_2$  datalogger (K-33 BLG,  $\text{CO}_2/\text{RH}+\text{temperature}$  datalogger, USA) and an  $\text{NH}_3$  sensor (4- $\text{NH}_3$ -100, Honeywell, USA) placed inside as reference sensors. The experiment was conducted at a temperature regulated laboratory with a temperature set as  $22^\circ\text{C}$ .

1) *Characterisation of  $\text{CO}_2$  Measurement*: The pH-sensitive dye, thymol blue forms ion-pairs with TMAH inside of the sol-gel matrix resulting in a deprotonated status, and the abundant

TMAH inside of the film act as a buffer solution that helps to maintain an alkaline environment [23]. The sensing of  $\text{CO}_2$  involves a  $\text{CO}_2$  hydration reaction by water molecules ( $\text{H}_2\text{O}$ ) of the ion-pairs described by:



where  $Q^+$  is a tetramethylammonium ion and  $T^-$  is the deprotonated thymol blue. The  $\text{CO}_2$  dissolves into the film and reacts with the hydrate water molecules of the ion pairs ( $Q^+T^- \bullet x\text{H}_2\text{O}$ ) forming carbonic acid ( $\text{H}_2\text{CO}_3$ ) which further dissociates into protons ( $\text{H}^+$ ) and bicarbonate ions ( $\text{HCO}_3^-$ ). The former protonates the thymol blue leading to a change of spectral property. Previous research demonstrated that a thymol blue and TMAH doped sol-gel film undergoes a colour transition from blue to yellow while interacting with  $\text{CO}_2$  resulting in a decrease of absorbance at  $\lambda = 608$  nm and an increase of absorbance around  $\lambda = 480$  nm [23].

For measuring  $\text{CO}_2$ , the chamber is initially filled with  $\text{N}_2$  gas (100%) and then the concentration of  $\text{CO}_2$  is gradually increased step-by-step via regulating the flow of  $\text{CO}_2$  (5% in argon mixture). Each step is maintained for at least 5 mins to obtain a stabilised signal for each concentration. The absorption spectrum of the fibre sensor is recorded simultaneously along with the readings from the commercial  $\text{CO}_2$  datalogger. In order to produce a rapid change in  $\text{CO}_2$  to measure the response time the fibre is placed directly from ambient ( $\sim 700$  ppm) into a chamber filled with  $\sim 5\%$   $\text{CO}_2$ . The relative humidity value inside of the measurement box is  $34.5 \pm 3.3\%$  across the measurement.

2) *Characterisation of  $\text{NH}_3$  Measurement:*  $\text{NH}_3$  gas inside the measurement chamber is generated from the evaporation of a drop of  $\text{NH}_4\text{OH}$  aqueous solution due to the existing equilibrium:



The sensing of gaseous  $\text{NH}_3$  by the OFS is determined by the TPPS which has intense absorption bands (Soret-band) at around  $\lambda = 420\text{--}480$  nm and a weaker band (Q-band) in the region of  $\lambda = 500\text{--}700$  nm [25]. The exact absorption peak depends on the aggregated state of molecules accommodated in the film [25], [26]. Spectral change of TPPS in the film is induced by polar effects: protonation and electronic interaction with matrix materials; and interactions between TPPS molecules. The TPPS molecule undergoes a deprotonation process induced by interaction with  $\text{NH}_3$  (illustrated in Fig. 2). As a result, deprotonation leads to the disruption of J-aggregation and the absorption spectrum is changed [26], [27].

The concentration of gaseous ammonia inside the chamber is generated by adding different volumes (2  $\mu\text{L}$ , 4  $\mu\text{L}$ , 8  $\mu\text{L}$ , 16  $\mu\text{L}$ , 32  $\mu\text{L}$  and 64  $\mu\text{L}$ ) of 1% ammonium hydroxide ( $\text{NH}_4\text{OH}$ ) solutions on a glass substrate (reservoir) inside the chamber. Each solution is retained for about 6 mins to reach equilibrium between the released gaseous  $\text{NH}_3$  and the  $\text{NH}_4\text{OH}$  reservoir (as indicated by the commercial  $\text{NH}_3$  sensor).

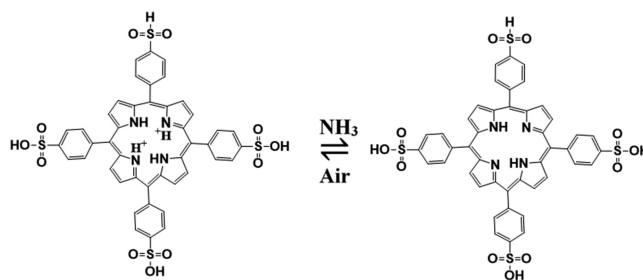


Fig. 2. Translational change of a TPPS molecule under an  $\text{NH}_3$  atmosphere. The TPPS molecule undergoes deprotonation of porphyrins ring while interacting with  $\text{NH}_3$ .

The cap is then opened and the reservoir removed to bring the concentration back to ambient level (0 ppm). The optical signal is recorded in real-time during the measurement and a commercial  $\text{NH}_3$  sensor records the concentration inside the chamber for reference. The  $\text{NH}_3$  response and recovery time is conducted in a separate test by quickly exposing the sensor to  $\text{NH}_3$  ( $\sim 35$  ppm) and removing the sensor back to the ambient level.

3) *The measurement in a Complex Gas Environment:* For investigating the feasibility of the OFS working in a complex gas atmosphere containing other volatile organic compounds (VOCs), the gas chamber that hosts the OFS is initially filled with  $\sim 60000$  ppm of  $\text{CO}_2$  for 10 mins, followed by adding 20  $\mu\text{L}$  methanol and acetone to the sealed chamber and waiting for another 10 mins. After allowing both methanol and acetone to evaporate, the chamber contains  $\sim 60000$  ppm  $\text{CO}_2$ , 33,577 ppm methanol and 18,336 ppm acetone (the methanol/acetone concentration is calculated based on the ideal gas law). Then 10  $\mu\text{L}$  of 1%  $\text{NH}_4\text{OH}$  solution is added into the gas chamber, which generates an additional  $\text{NH}_3$  gas vapour (concentration is  $\sim 3.5$  ppm from the reading of commercial sensor). The final gas mixture is composed of  $\text{CO}_2$ , methanol, acetone and  $\text{NH}_3$ . The relative humidity inside of the measurement chamber during the measurement process remains relatively stable at  $28.5 \pm 3.9\%$ .

The absorbance value for a specific wavelength ( $\lambda$ ) is determined as the logarithm of the ratio of the reflected intensity from the coated fibre,  $I(\lambda)$ , to the reflected intensity measured prior to film deposition,  $I_0(\lambda)$ :

$$A(\lambda) = -\log \frac{I(\lambda)}{I_0(\lambda)} \quad (3)$$

The limit of detection (LOD) is defined as three times the standard deviation ( $\delta$ ) of the signal at a constant concentration divided by the sensitivity that is the slope of the linear region of the relationship between the analyte and light intensity [28].

$$\text{LOD} = \frac{3 \times \delta}{S} \quad (4)$$

The response time and recovery time are defined as the time between 10% to 90%, and 90% to 10% of the signal change when the signal jumps from one stable value to another stable value as response to the change of the presence of analyte.

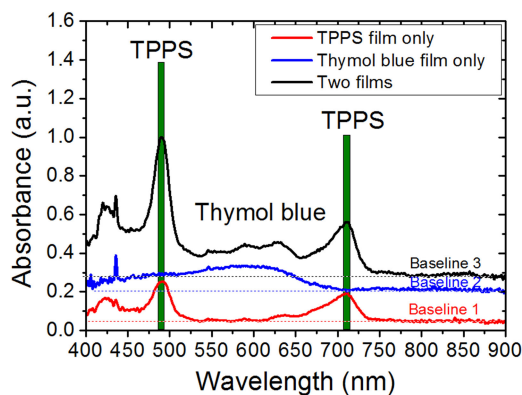


Fig. 3. Absorption spectrum after coating the two tips of an optical fibre coupler with a TPPS film and a thymol blue film.

### III. RESULTS

The MTEOS undergoes hydrolysis and condensation during the sol-gel reaction that forms the backbone of the gel network but also ensures strong chemical adhesion to the glass fibre. The TMAH and HCl added in each sol-gel preparation act as an alkaline and acidic catalyst for accelerating the reaction meanwhile activate the dyes in the appropriate deprotonation/protonation status for sensing of  $\text{CO}_2$  and  $\text{NH}_3$ .

Fig. 3 illustrates the absorption spectrum of the OFS after being coated with the gas-sensitive films. The spectrum presents three distinctive peaks at  $\lambda = 420$  nm, 490 nm and 711 nm after coating one tip of the optical fibre coupler with TPPS film and leaving the other uncoated (red line, Fig. 3). The absorption features are in agreement with the observation in the previously published work [24]. A new absorption peak around  $\lambda = 608$  nm appears after coating the second tip with the film doped with thymol blue and phase transfer agent (TMAH) (blue line, Fig. 3). This is due to the absorption of the deprotonated thymol blue [23]. The increased baseline in the spectrum is attributed to the attenuation of the sol-gel matrix film. The distinctive absorption features from the two sensitive films render the possibility of sensing multiple analytes by monitoring the absorption change (black line, Fig. 3).

#### A. Measurement of Gasous $\text{CO}_2$

Fig. 4a shows the absorption spectrum of the OFS at 0 ppm and  $\sim 60000$  ppm of  $\text{CO}_2$  atmosphere. The absorbance value in the region around  $\lambda = 608$  nm decreases at  $\text{CO}_2$  atmosphere and the other two peaks remain relatively stable. Fig. 4b shows the dynamic change of absorbance at  $\lambda = 608$  nm during the  $\text{CO}_2$  measurement in comparison to the reading of the commercial  $\text{CO}_2$  datalogger. The absorbance value shows a decrease as the  $\text{CO}_2$  concentration raises step by step from 0 ppm to 60000 ppm. The average absorption value of each step exhibits an exponential correlation ( $R^2 = 0.99$ ) to the concentration of  $\text{CO}_2$  (Fig. 4c). Within the detected range, the absorbance value shows a linear correlation for the  $\text{CO}_2$  concentration in the range from 0 ppm to  $\sim 20,000$  ppm with a sensitivity of  $-1.6 \times 10^{-6}/\text{ppm}$  (inner graph of Fig. 4c,  $R^2 = 0.96$ ). The LOD is calculated as

637 ppm using Equation (4). The absorbance changes of three wavelengths: 490 nm, 711 nm and 608 nm corresponding to different concentrations of  $\text{CO}_2$  are illustrated in Fig. 4d. As a contrast, the absorbance value at  $\lambda = 711$  nm that is from absorption of TPPS exhibits almost no change to  $\text{CO}_2$  in the tested range. However, another absorbance value of TPPS at  $\lambda = 490$  nm increases with the increase of  $\text{CO}_2$  concentration. This change is due to the overlapping of the absorption peak with that of thymol blue around  $\lambda = 480$  nm and the increase of absorbance is caused by thymol blue rather than TPPS. The absorbance at  $\lambda = 608$  nm is also reversible as  $\text{CO}_2$  concentration decreases (illustrated in Fig. 4e). The response and recovery time is calculated as 86 s and 236 s, respectively.

#### B. Measurement of Gasous $\text{NH}_3$

The spectral response of the OFS to  $\text{NH}_3$  is illustrated in Fig. 5a in which the two bands (Soret band and Q-band) show a decrease in the absorbance value whereas the  $\text{CO}_2$  sensitive region (around  $\lambda = 608$  nm) remains unchanged. Fig. 5b shows the dynamic response of absorbance of the two absorption peaks ( $\lambda = 490$  nm and 711 nm) of the OFS to different concentrations of  $\text{NH}_3$  from 0 ppm up to 80 ppm. The two wavelengths exhibit a reversible decrease in their absorbance value in response to  $\text{NH}_3$ . The relationship between absorbance at  $\lambda = 711$  nm to the concentration of  $\text{NH}_3$  is shown in Fig. 5c where an exponential fitting is employed ( $R^2 = 0.96$ ) for the detected concentration range. Its sensitivity and LOD are defined as  $-0.00672/\text{ppm}$  and 0.15 ppm respectively based on the linear fitting of the first four concentrations in the concentration range from 0 ppm up to 4 ppm (inner graph in Fig. 5c,  $R^2 = 0.87$ ). The response time and recovery time is calculated as 83 s and 363 s respectively from Fig. 5e where the sensor is quickly exposed to  $\sim 35$  ppm of  $\text{NH}_3$  from an ambient concentration.

Although the absorbance shows a bigger change at  $\lambda = 490$  nm than that at  $\lambda = 711$  nm in response to  $\text{NH}_3$  (illustrated in Fig. 5d), the interference to  $\text{CO}_2$  of the absorbance at 490 nm as shown in Fig. 4d demonstrates that the cross sensitivity means it is not the optimum wavelength for indicating  $\text{NH}_3$  concentration in a  $\text{CO}_2$  atmosphere. The absorbance at  $\lambda = 711$  nm is therefore used to indicate  $\text{NH}_3$  concentration.

Apart from absorption change, the wavelength of the absorption peaks also shifts in response to  $\text{NH}_3$  as illustrated in Fig. 6a. The two bands shift in opposite directions as the  $\text{NH}_3$  concentration increases, the Q-band undergoes a blue shift while the Soret band shifts to a longer wavelength. The Soret band also shows a broadening of the absorbance peak with an increase of  $\sim 4$  nm at 12 ppm  $\text{NH}_3$  of the full width at half maximum (FWHM). The red shift and broadening of the Soret band and blue shift of Q bands of TPPS have been reported as a result of forming a complex with other chemicals due to aggregate structure change [26], in this case, a TPPS- $\text{NH}_3$  complex. The magnitude of the wavelength shift is illustrated in Fig. 6b in which the Q-band has a larger shift in response to a concentration of  $\text{NH}_3$  in the detected range. Due to the opposite change of the dual bands, the distance between the two bands can also be applied for indicating the

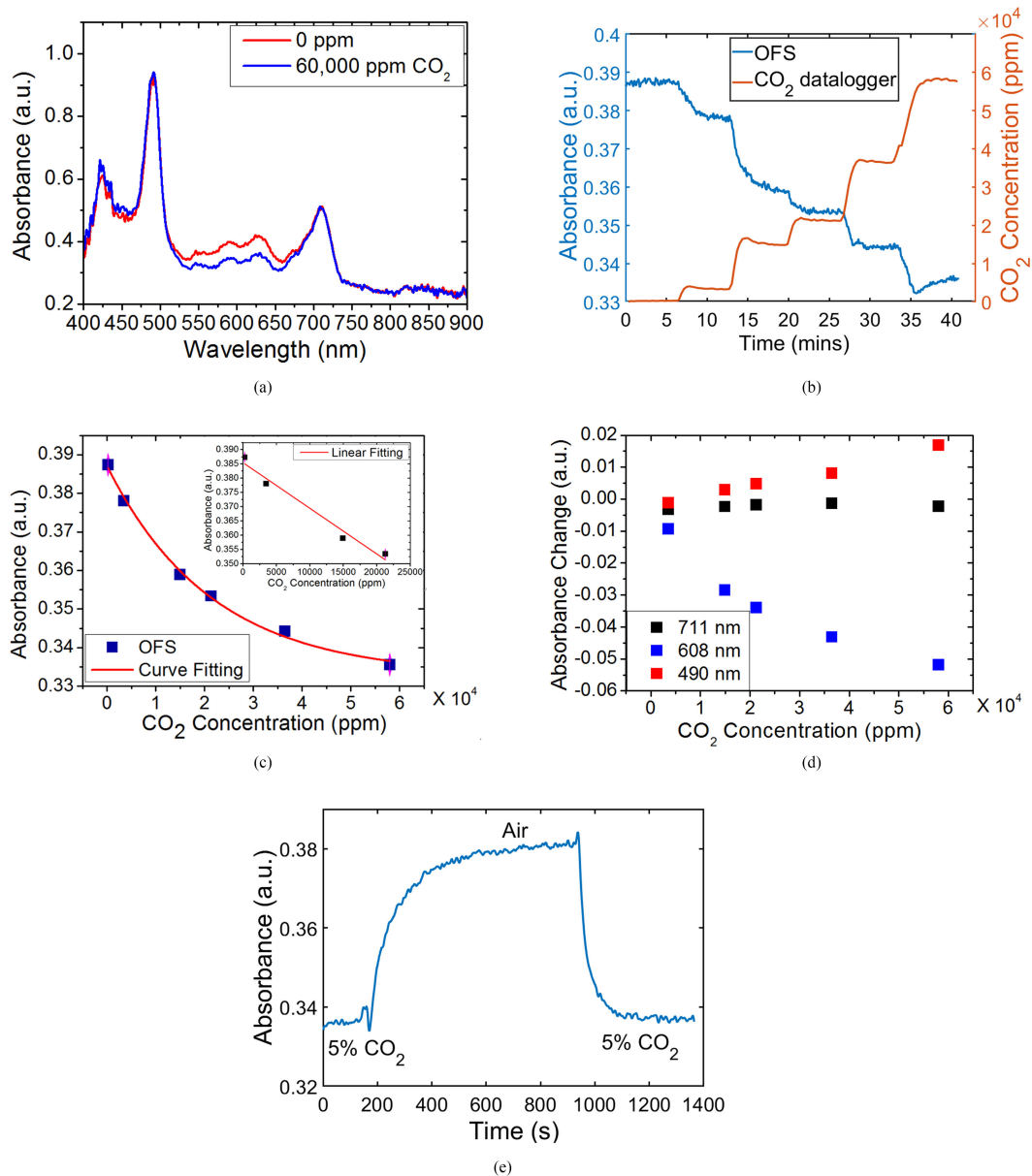


Fig. 4. (a) Spectral response of the OFS to  $\text{CO}_2$ . (b) The response of absorbance value at  $\lambda = 608$  nm to the change of  $\text{CO}_2$  concentration. (c) The absorbance value against the concentration of  $\text{CO}_2$ . Each point in the graph is the average value of each step in (b). Error bars are smaller than marker size. The inner graph shows the linear fitting of the first four concentrations. (d) The comparison of three wavelengths in response to different concentration of  $\text{CO}_2$ . (e) The reversible response of absorbance value ( $\lambda = 608$  nm) to  $\text{CO}_2$ .

$\text{NH}_3$  concentration. It shows a larger wavelength shift than the single band with a sensitivity of  $-0.7$  nm/ppm for the linear range from 0 ppm up to 4 ppm ( $R^2 = 0.86$ ). Using Equation (4), the LOD is 0.2 ppm, which is slightly bigger than that obtained using absorbance values (0.15 ppm). The wavelength-shift based method provides an advantage of tolerating drift of light intensity over the absorbance based method for long-term application. Another way of compensating the intensity drift is by using a reference wavelength to subtract the drift. The reference wavelength should not be sensitive to the target analyte. This method is significant in the  $\text{CO}_2$  measurement as it does not exhibit a wavelength shift. The reference wavelength in this case can be selected between 750 nm to 900 nm. In terms of

instrument miniaturisation, the absorbance-based method can be measured with low-cost photodetectors, whereas the wavelength-shift measurement requires a more complicated spectrometer-like configuration that raises the complexity and cost of the hardware.

Table I lists the key features of the proposed OFS by using absorption based measurement for the sensing of  $\text{CO}_2$  and  $\text{NH}_3$  compared to the previously reported OFSs. The proposed sensor shows the unique feature of sensing both parameters simultaneously with comparable response time and better LOD than the previously reported. The lower LOD enables the sensor to be applied in monitoring the air quality of workspaces where both gases are considered such as farmland, livestock feeding

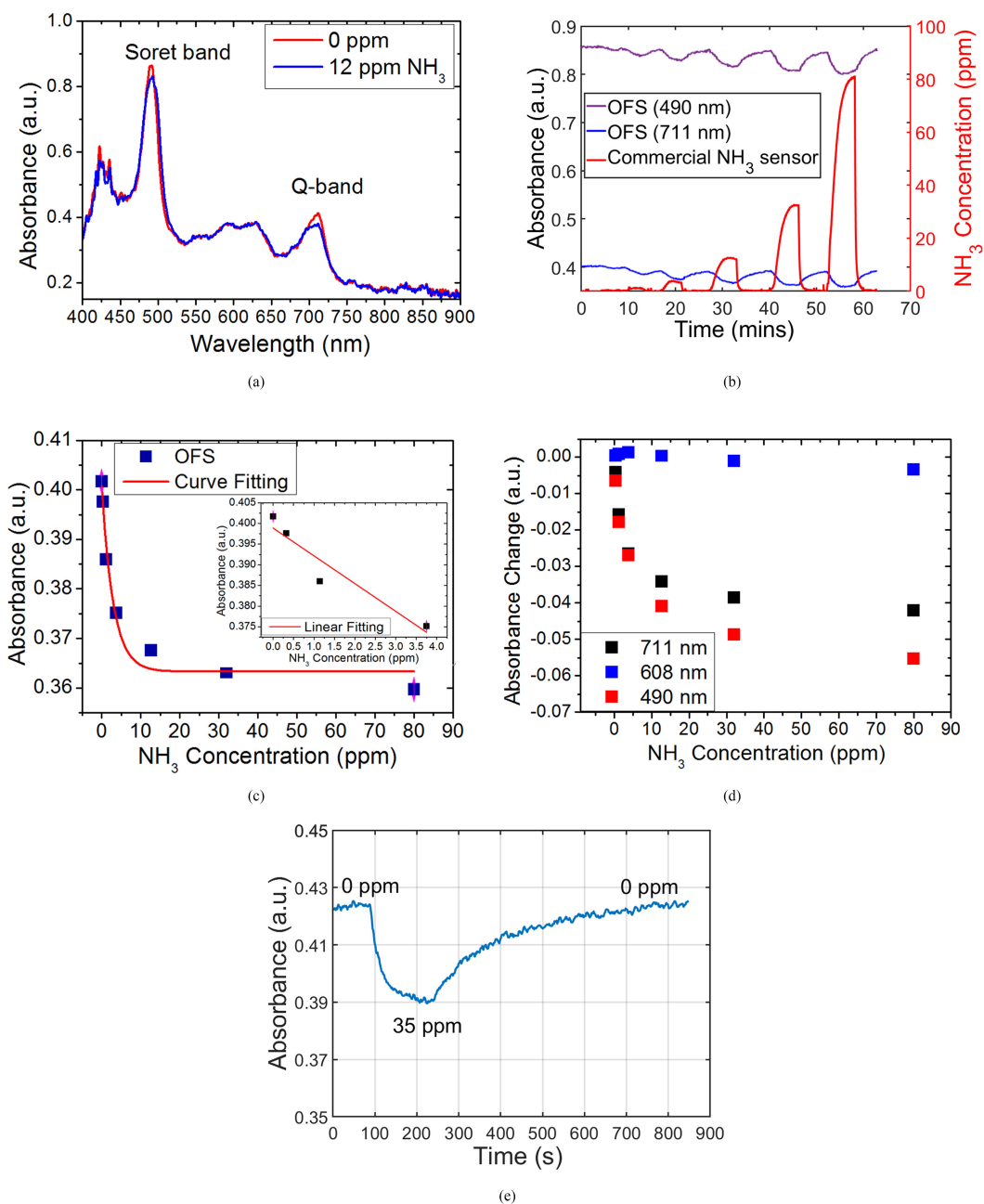
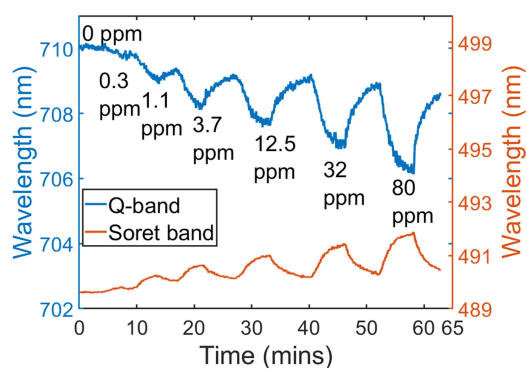


Fig. 5. (a) Spectral response of OFS to  $\text{NH}_3$ . (b) The absorbance value of OFS at the two different wavelengths (490 and 711 nm) in response to  $\text{NH}_3$  concentration. (c) Exponential fitting of absorbance value at 711 nm to the concentration of  $\text{NH}_3$ . The inner graph illustrates the linear fitting for the first four points in the concentration range up to 4 ppm. (d) The change of absorbance value at three different wavelengths against  $\text{NH}_3$  concentration. (e) The response time of OFS to  $\text{NH}_3$  with a concentration of  $\sim 35$  ppm.

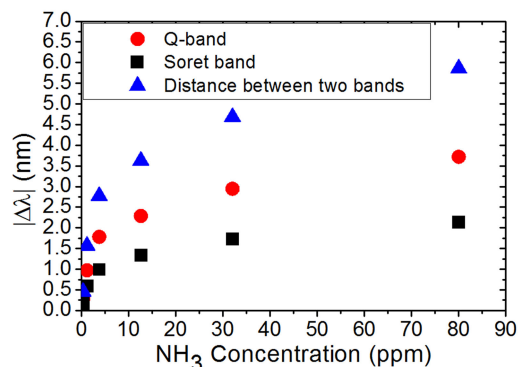
industry or fertiliser manufacturing industry and the application in healthcare for breath gas analysis.

Humidity in breath gas is a major adverse factor to the sensing performance due to the water condensation on the sol-gel film. At a high humidity condition ( $>70\%$ ), the reflection intensity undergoes a drop as a result of water adsorption due to the increase of the refractive index. This is consistent with results demonstrated previously [23]. In our previous publication [23], breath  $\text{CO}_2$  is accurately measured by using the optical fibre

$\text{CO}_2$  sensor after passing through a home-made humidity filter. The proposed  $\text{NH}_3$  and  $\text{CO}_2$  dual sensor in this article are suggested to be covered with a semipermeable membrane such as polytetrafluoroethylene (PTFE) membrane which allows the permeation of gases and prevents water condensation as it tends to neutralize the pH of film. Temperature does not have a significant effect on the absorbance value of the dyes ( $<1.5\%$  change in absorbance over the range  $25^\circ\text{C}$  to  $40^\circ\text{C}$ ). However, the  $\text{CO}_2$  reaction in Equation (1) is a temperature dependent and



(a)



(b)

Fig. 6. (a) Central wavelength of two bands in response to  $\text{NH}_3$ . (b) Absolute wavelength shift corresponding to the concentration of  $\text{NH}_3$ .

TABLE I  
THE COMPARISON OF THE PROPOSED SENSOR TO THE PREVIOUSLY PUBLISHED OFSS

OFS	analyte	Sensing platform	Sensing materials	LOD (ppm)	Response time (s)
Proposed sensor	$\text{CO}_2$	Fibre tip	Thymol blue	637	86
	$\text{NH}_3$	Fibre tip	TPPS	0.15	83
Ref. [29]	$\text{CO}_2$	u-shape fibre	Phenol red	6,500	2-3
Ref. [30]	$\text{CO}_2$	HC-PCF	Infrared absorption	20,000	600
Ref. [31]	$\text{CO}_2$	LPG	HKUST-1	401	260
Ref. [32]	$\text{NH}_3$	u-shape fibre	Bromocresol purple	10	10
Ref. [33]	$\text{NH}_3$	Side-poli shed fibre	Graphene/polyaniline	22.46	112
Ref. [34]	$\text{NH}_3$	Fibre tip	Fluorescent aza-BODIPY	< 43	> 30

HC = Hollow core; PCF = Photonic-crystal fibre.

such an exothermic reaction leads to a lower sensitivity at high temperature as shown in Fig. 7, which is more pronounced for higher ( $>1\%$ )  $\text{CO}_2$  concentration. The absorption change within  $5^\circ\text{C}$  in the range of  $30\text{--}35^\circ\text{C}$  is minor and would be suitable for the sensing applications in healthcare. Therefore, the sensor can be treated as temperature insensitive where the temperature fluctuation is small. For other applications where temperature change is more pronounced, temperature effect would need to be compensated for using an additional temperature sensor [35].

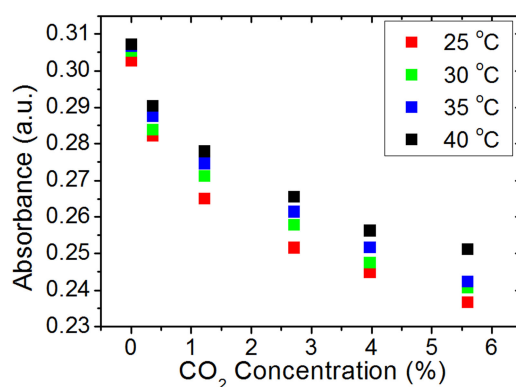


Fig. 7. The measurement of  $\text{CO}_2$  at different temperature.

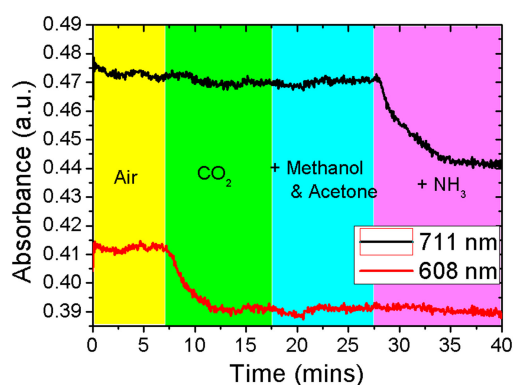


Fig. 8. Dynamic response of the OFS to a mixture of gases containing  $\text{CO}_2$  ( $\sim 60,000$  ppm), methanol (33,577 ppm), acetone (18,336 ppm) and  $\text{NH}_3$  (3.5 ppm). The concentrations of  $\text{CO}_2$  and  $\text{NH}_3$  are directly read from the commercial sensor and concentration of methanol and acetone are calculated based on the ideal gas law.

### C. Simultaneous Measurement of $\text{CO}_2$ and $\text{NH}_3$ in a Complex Gas Atmosphere

Specificity, the ability to detect the analyte of interest in a complex matrix, is an important parameter of any chemical or biosensor. In order to study the sensors' specificity their responses in an environment containing a mixture of  $\text{CO}_2$ , methanol, acetone and  $\text{NH}_3$  was studied and results are shown in Fig. 8. The absorbance of the wavelength changes dynamically as the gases supplied change. Methanol and acetone are two of other VOCs presented in breath apart from  $\text{CO}_2$  and  $\text{NH}_3$  [18]. The absorbance value at  $\lambda = 608$  nm decreases while  $\text{CO}_2$  is infused into the gas chamber and remains stable at the  $\text{CO}_2$  concentration inside of chamber remains the same as  $\sim 60,000$  ppm which is shown by the commercial datalogger (7–17 mins in Fig. 8).

The absorbance value at  $\lambda = 711$  nm remains unchanged after the infusion of  $\text{CO}_2$  compared to its value in ambient air. Both wavelengths show no response to the methanol and acetone vapour (17–27 mins in Fig. 8) demonstrating negligible cross-sensitivity to the tested VOCs. The wavelength of 711 nm starts to decrease at the time at about 27 mins when  $\text{NH}_4\text{OH}$

was added into the chamber. It gradually decreases and finally stabilised in the next 10 mins in response to the equilibrium of gaseous  $\text{NH}_3$  in the chamber (concentration of 3.5 ppm). The wavelength of 608 nm, on the other hand, remains constant due to negligible  $\text{NH}_3$  cross sensitivity as discussed later. The sensor test in the mixture of gases demonstrates the capability of the OFS to measure  $\text{CO}_2$  and  $\text{NH}_3$  simultaneously and the presence of VOCs, i.e., methanol and acetone, do not interfere with the sensor response.

#### IV. DISCUSSION

The two dye compounds used for sensing of  $\text{CO}_2$  and  $\text{NH}_3$  in the above experiment are pH dependent. The  $\text{CO}_2$  sensitive dye (thymol blue) can only work in the presence of alkaline phase transfer (TMAH). The  $\text{NH}_3$  sensitive dye (TPPS), however, operates only when the pH is neutral or acidic. Therefore, the spectrum in Fig. 3 which contains the absorption region for both  $\text{NH}_3$  and  $\text{CO}_2$  sensing cannot be obtained by doping the two dyes into one matrix film (results not shown). In other words, the combination of the two dyes into one matrix film for the simultaneous measurement of  $\text{CO}_2$  and  $\text{NH}_3$  cannot be achieved due to the pH uniformity of one single film. As one film cannot survive in the other's coating solution due to different pH value, a two-film structure with one on the top of another cannot be obtained via the dip coating method (data not shown).

The sensing of  $\text{CO}_2$  and  $\text{NH}_3$  is a process of protonation and deprotonation of the relevant dye. The  $\text{CO}_2$  is an acidic gas, and it reacts with the hydrate water molecules forming carbonic acids, which are the proton donor to the thymol blue. However, the majority of  $\text{CO}_2$  (more than 99%) in water exists as the dissolved gas and less than 1% as carbonic acid [36]. In the  $\text{CO}_2$  sensing film, the doping of alkaline phase transfer (TMAH) provides abundant hydrate molecule due to the formation of ion-pair with the dye and the equilibrium in Equation (1) shifts to the right side, and as a result, more dissolved  $\text{CO}_2$  is converted into carbonic acid. Besides, the abundant base doped in the film also provides a higher pH that enhances the solubility of  $\text{CO}_2$  as a result of the shift in the equilibrium. When it comes to the  $\text{NH}_3$  sensing film, the ambient water molecules that react to  $\text{CO}_2$  are not enough to produce sufficient protons to change the spectral property of the TPPS leading to a negligible response to  $\text{CO}_2$ .

On the other hand,  $\text{NH}_3$  is an alkaline gas and acts as a proton receptor that deprotonates the TPPS molecule. Its solubility is very low in a high pH value of water medium due to inhibition of the dissociation of ammonia hydroxide in Equation (2). As a result, diffusion of  $\text{NH}_3$  into the  $\text{CO}_2$  sensitive film is very low leading to negligible cross-sensitivity of  $\text{NH}_3$ .

#### V. CONCLUSION

Multi-parameter sensing of  $\text{CO}_2$  and  $\text{NH}_3$  is achieved by using an optical fibre sensor fabricated by separately coating two dyes (thymol blue and TPPS) on the two distal ends of a  $2 \times 2$  optical fibre coupler. The distinctive absorption features of the two dyes at the reflection spectrum facilitates independent responses of

the optical signals to  $\text{CO}_2$  and  $\text{NH}_3$ . Two absorption peaks positioned at  $\lambda = 608$  nm and 711 nm in the reflection spectrum are suitable for sensing of  $\text{CO}_2$  and  $\text{NH}_3$  with negligible cross-talk between each measurement. Their absorbance value decreases in response to the increase of  $\text{CO}_2$  and  $\text{NH}_3$ . The LOD for sensing of  $\text{CO}_2$  and  $\text{NH}_3$  is 637 ppm and 0.15 ppm.

The reported sensor demonstrates the capability of sensing  $\text{CO}_2$  and  $\text{NH}_3$  with no interference with each measurement and is capable of sensing the two gases simultaneously with negligible cross-sensitivity to tested VOCs i.e., methanol and acetone.

#### REFERENCES

- [1] M. Pospíšilová, G. Kuncová, and J. Trögl, "Fiber-optic chemical sensors and fiber-optic bio-sensors," *Sensors*, vol. 15, no. 10, pp. 25208–25259, 2015.
- [2] A. Kharaz and B. E. Jones, "A distributed optical-fibre sensing system for multi-point humidity measurement," *Sensors Actuators A, Phys.*, vol. 47, no. 1, pp. 491–493, 1995.
- [3] R. B. Thompson, "Fluorescence-based fiber-optic sensors," in *Topics in Fluorescence Spectroscopy: Principles*, J. R. Lakowicz, Ed. Boston, MA, USA: Springer, 2002, pp. 345–365.
- [4] L. Liu *et al.*, "Highly sensitive label-free antibody detection using a long period fibre grating sensor," *Sensors Actuators B, Chem.*, vol. 271, pp. 24–32, 2018.
- [5] R. Correia, S. James, S. Lee, S. Morgan, and S. Korposh, "Biomedical application of optical fibre sensors," *J. Opt.*, vol. 20, no. 7, 2018, Art. no. 073003.
- [6] G. Whitenett, G. Stewart, K. Atherton, B. Culshaw, and W. Johnstone, "Optical fibre instrumentation for environmental monitoring applications," *J. Opt. A, Pure Appl. Opt.*, vol. 5, no. 5, 2003, Art. no. S140.
- [7] M. Uttamall and D. R. Walt, "A fiber-optic carbon dioxide sensor for fermentation monitoring," *Bio/Technol.*, vol. 13, no. 6, pp. 597–601, 1995.
- [8] P. Kronenberg, P. K. Rastogi, P. Giaccari, and H. G. Limberger, "Relative humidity sensor with optical fiber Bragg gratings," *Opt. Lett.*, vol. 27, no. 16, pp. 1385–1387, 2002.
- [9] J. Hromadka *et al.*, "Multi-parameter measurements using optical fibre long period gratings for indoor air quality monitoring," *Sensors Actuators B, Chem.*, vol. 244, pp. 217–225, 2017.
- [10] L. Li and D. R. Walt, "Dual-analyte fiber-optic sensor for the simultaneous and continuous measurement of glucose and oxygen," *Analytical Chem.*, vol. 67, no. 20, pp. 3746–3752, 1995.
- [11] B. Sciacca and T. M. Monro, "Dip biosensor based on localized surface plasmon resonance at the tip of an optical fiber," *Langmuir*, vol. 30, no. 3, pp. 946–954, 2014.
- [12] K. J. Donham, "Association of environmental air contaminants with disease and productivity in swine," *Amer. J. Veterinary Res.*, vol. 52, no. 10, pp. 1723–1730, 1991.
- [13] C. Charavaryamath and B. Singh, "Pulmonary effects of exposure to pig barn air," *J. Occupational Med. Toxicol.*, vol. 1, no. 1, 2006, Art. no. 10.
- [14] N. Roney and F. Lladós, "Toxicological profile for ammonia," Agency for Toxic Substances and Disease Registry, Syracuse Research Corp., U.S. Dept. Health Human Services, Atlanta, GA, 2004.
- [15] S. Davies, P. Spanel, and D. Smith, "Quantitative analysis of ammonia on the breath of patients in end-stage renal failure," *Kidney Int.*, vol. 52, no. 1, pp. 223–228, 1997.
- [16] J. H. Shorter, D. D. Nelson, J. B. McManus, M. S. Zahniser, S. R. Sama, and D. K. Milton, "Clinical study of multiple breath biomarkers of asthma and COPD ( $\text{NO}$ ,  $\text{CO}_2$ ,  $\text{CO}$  and  $\text{N}_2\text{O}$ ) by infrared laser spectroscopy," *J. Breath Res.*, vol. 5, no. 3, 2011, Art. no. 037108 (in English).
- [17] J. G. Kusters, A. H. van Vliet, and E. J. Kuipers, "Pathogenesis of *Helicobacter pylori* infection," *Clin. Microbiol. Rev.*, vol. 19, no. 3, pp. 449–490, 2006.
- [18] C. Lourenço and C. Turner, "Breath analysis in disease diagnosis: Methodological considerations and applications," *Metabolites*, vol. 4, no. 2, pp. 465–498, 2014.
- [19] A. Amann, G. Poupart, S. Telser, M. Ledochowski, A. Schmid, and S. Mechtcheriakov, "Applications of breath gas analysis in medicine," *Int. J. Mass Spectrometry*, vol. 239, no. 2–3, pp. 227–233, 2004.
- [20] W. Cao and Y. Duan, "Current status of methods and techniques for breath analysis," *Crit. Rev. Analytical Chem.*, vol. 37, no. 1, pp. 3–13, 2007.

- [21] K. Wysokiński, M. Napierała, T. Stańczyk, S. Lipiński, and T. Nasiłowski, "Study on the sensing coating of the optical fibre CO<sub>2</sub> sensor," *Sensors*, vol. 15, no. 12, pp. 31888–31903, 2015.
- [22] A. Rodríguez, C. Zamarreño, I. Matías, F. Arregui, R. Cruz, and D. May-Arrijoja, "A fiber optic ammonia sensor using a universal pH indicator," *Sensors*, vol. 14, no. 3, pp. 4060–4073, 2014.
- [23] L. Liu, F. Hao, S. P. Morgan, R. Correia, A. Norris, and S. Korposh, "A reflection-mode fibre-optic sensor for breath carbon dioxide measurement in healthcare," *Sens. Bio-Sens. Res.*, vol. 22, 2019, Art. no. 100254.
- [24] S. Korposh, S. Kodaira, W. Batty, S. W. James, and S.-W. Lee, "Nanoassembled thin-film gas sensor II. An intrinsic highly sensitive fibre-optic sensor for ammonia detection," *Sensors Mater.*, vol. 21, no. 4, pp. 179–189, 2009.
- [25] R. Selyanchyn, S. Korposh, W. Yasukochi, and S.-W. Lee, "A preliminary test for skin gas assessment using a porphyrin based evanescent wave optical fiber sensor," *Sensors Transducers*, vol. 125, no. 2, pp. 54–67, 2011.
- [26] S. Takagi, M. Eguchi, D. A. Tryk, and H. Inoue, "Porphyrin photochemistry in inorganic/organic hybrid materials: Clays, layered semiconductors, nanotubes, and mesoporous materials," *J. Photochem. Photobiol. C, Photochemistry Rev.*, vol. 7, no. 2, pp. 104–126, 2006.
- [27] K. Ariga, Y. Lvov, and T. Kunitake, "Assembling alternate dye–polyion molecular films by electrostatic layer-by-layer adsorption," *J. Amer. Chem. Soc.*, vol. 119, no. 9, pp. 2224–2231, 1997.
- [28] A. Shrivastava and V. B. Gupta, "Methods for the determination of limit of detection and limit of quantitation of the analytical methods," *Chronicles Young Scientists*, vol. 2, no. 1, pp. 15–21, 2011.
- [29] K. Wysokiński, M. Napierała, T. Stańczyk, S. Lipiński, and T. Nasiłowski, "Study on the sensing coating of the optical fibre CO<sub>2</sub> sensor," *Sensors*, vol. 15, no. 12, pp. 31888–31903, 2015.
- [30] S. M. Mejia Quintero, L. C. Guedes Valente, M. S. de Paula Gomes, H. Gomes da Silva, B. Caroli de Souza, and S. R. K. Morikawa, "All-fiber CO<sub>2</sub> sensor using hollow core PCF operating in the 2 μm region," *Sensors Basel, Switzerland*, vol. 18, no. 12, 2018, Art. no. 4393.
- [31] J. Hromadka, B. Tokay, R. Correia, S. P. Morgan, and S. Korposh, "Carbon dioxide measurements using long period grating optical fibre sensor coated with metal organic framework HKUST-1," *Sensors Actuators B, Chem.*, vol. 255, pp. 2483–2494, 2018.
- [32] W. Cao and Y. Duan, "Optical fiber-based evanescent ammonia sensor," *Sensors Actuators B, Chem.*, vol. 110, no. 2, pp. 252–259, 2005.
- [33] A. L. Khalaf *et al.*, "Room temperature ammonia sensor using side-polished optical fiber coated with graphene/polyaniline nanocomposite," *Opt. Mater. Exp.*, vol. 7, no. 6, pp. 1858–1870, 2017.
- [34] M. Maierhofer, S. M. Borisov, and T. Mayr, "Optical ammonia sensor for continuous bioprocess monitoring," *Proceedings*, vol. 2, no. 13, 2018, Art. no. 1041.
- [35] C. He, S. Korposh, R. Correia, B. R. Hayes-Gill, and S. P. Morgan, "Optical fibre temperature sensor based on thermochromic liquid crystal," *Proc. SPIE*, vol. 11199, 2019, Art. no. 1119908.
- [36] W. Knoche, *Chemical Reactions of CO<sub>2</sub> in Water*, Berlin, Germany: Springer, 1980, pp. 3–11.

**LiangLiang Liu** received the Ph.D. degree from the Electrical and Electronic Engineering Department, University of Nottingham, Nottingham, U.K., in 2019. He is currently a Research Fellow in optics and photonics with the University of Nottingham. His research interest is to develop in vivo optical fibre bio-/chemical sensors.

**Stephen P. Morgan** is a Professor of biomedical engineering, University of Nottingham, Nottingham, U.K. Since 1992, he has investigated novel optical techniques for imaging and spectroscopy of tissue using laser Doppler flowmetry, acousto-optic imaging and hyperspectral imaging. His research involves the development of devices to monitor the microcirculation specifically in tissue breakdown and wound healing. For example, he is currently developing a novel endotracheal tube that can monitor the microcirculation at the cuff/trachea interface. His recent work involves the integration of optical fibre sensors into textiles. These sensing systems, incorporated into garments, can monitor pressure, temperature, and the microcirculation.

**Ricardo Correia**, biography not available at the time of publication.

**Seung-Woo Lee**, biography not available at the time of publication.

**Serhiy Korposh** received the bachelor's and master's degrees in physics from Uzhgorod National University, Transcarpathia, Ukraine, in 2001 and 2002, respectively, and the Ph.D. degree from Cranfield University, Bedford, U.K., in 2007. He was a Postdoctoral Researcher on development of the novel materials for chemical sensors with the Graduate School of Environmental Engineering, University of Kitakyushu, Japan, from 2008 to 2012. From 2012 to 2013, he was a Research Fellow with the Department of Engineering Photonics, Cranfield University. He is currently a Lecturer with the University of Nottingham, Nottingham, U.K. His research interest lies in the field of application and development of fiber-optic chemical sensors modified with the sensitive materials.